

ChemComm

Accepted Manuscript



This is an *Accepted Manuscript*, which has been through the Royal Society of Chemistry peer review process and has been accepted for publication.

Accepted Manuscripts are published online shortly after acceptance, before technical editing, formatting and proof reading. Using this free service, authors can make their results available to the community, in citable form, before we publish the edited article. We will replace this *Accepted Manuscript* with the edited and formatted *Advance Article* as soon as it is available.

You can find more information about *Accepted Manuscripts* in the [Information for Authors](#).

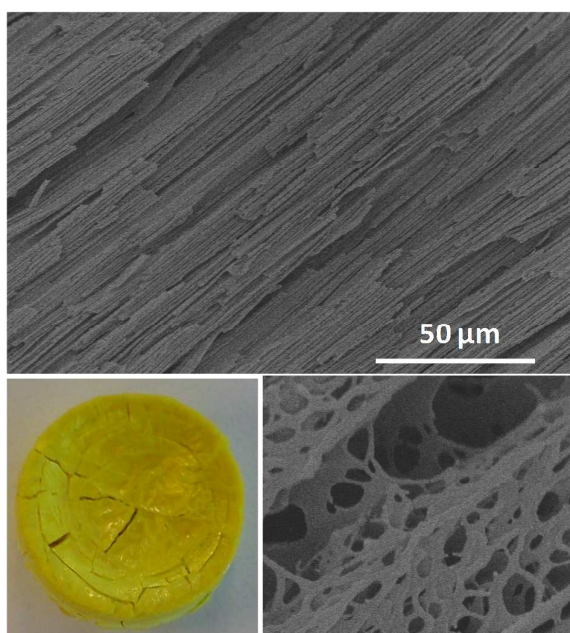
Please note that technical editing may introduce minor changes to the text and/or graphics, which may alter content. The journal's standard [Terms & Conditions](#) and the [Ethical guidelines](#) still apply. In no event shall the Royal Society of Chemistry be held responsible for any errors or omissions in this *Accepted Manuscript* or any consequences arising from the use of any information it contains.

ToC Graph

Title: Aligned macroporous monoliths with intrinsic microporosity via a frozen-solvent-templating approach

Authors: Adham Ahmed, Tom Hasell, Rob Clowes, Peter Myers, Andrew I Cooper and Haifei Zhang*

Abstract: Aligned macroporous monoliths of organic cage, polymer of intrinsic microporosity (PIM-1), and metal-organic framework (HKUST-1) are prepared by a controlled freezing approach. In addition to macropores, all the monoliths contain the intrinsic micropores.



COMMUNICATION

Aligned macroporous monoliths with intrinsic microporosity via a frozen-solvent-templating approach

Cite this: DOI: 10.1039/x0xx00000x

Received 00th January 2012,
Accepted 00th January 2012

Adham Ahmed, Tom Hasell, Rob Clowes, Peter Myers, Andrew I. Cooper and Haifei Zhang*

DOI: 10.1039/x0xx00000x

www.rsc.org/

Aligned macroporous monoliths of organic cage, polymer of intrinsic microporosity (PIM-1), and metal-organic framework (HKUST-1) are prepared by a controlled freezing approach. In addition to macropores, all the monoliths contain the intrinsic micropores.

Microporous materials contain pores or voids with the sizes less than 2 nm. This usually leads to the materials with high surface area. Microporous materials have been widely used in gas storage, gas separation, and as support for catalysis, among others. Traditionally, zeolites, aerogels, and carbon have been known and widely used.¹⁻² In recent years, new types of microporous materials including hypercrosslinked polymers, polymers of intrinsic microporosity (PIMs), organic cage compounds, and metal-organic frameworks (MOFs) have been intensively investigated and explored for various applications.³⁻⁶ However, the micropore structure has its own limitation, *i.e.*, the limited mass transport, which can be significant for applications where liquid phase or large molecules are utilized. Rational design and synthesis based on the use of different sized monomers may be used for cage compounds and MOFs.^{4,6}

Most of the above mentioned microporous materials are generally produced as powders and sometimes as thin films. Apart from cage compounds (CCs) and PIMs,^{4,5} these materials are either crosslinked or frameworks and they do not dissolve in solvent without the structures being broken. This can cause difficulty in processing or shaping these materials. When forming a membrane or monolith from the particulate microporous materials, a binder and/or stabilizer will have to be used, which may compromise the properties of the microporous materials.^{7,8} A monolith may offer robustness, easy handling, low flow resistance, essential supports for catalysis & separation.^{9,10}

Processing soluble microporous materials (*e.g.* CCs and PIMs) and MOFs to generate the monoliths containing hierarchical pores can be very important. This type of materials may offer the advantage of monoliths, exciting properties from the micropores, and the enhanced mass transport due to the presence of mesopores and/or macropores. PIM membranes, with porous inorganic entities or

embedded CC crystals, can be readily prepared by solvent casting for enhanced gas separation.¹¹⁻¹³ MOF monoliths may be formed by compression densification of pre-formed MOF particles.¹⁴ MOF composite monoliths can be prepared by *in situ* formation/growth of MOF within a porous monolithic scaffold.¹⁰ The report on the formation of MOF monolith from precursors is very limited. Only two examples have been noticed, including the synthesis of zeolitic metal azolate framework¹⁵ and the HKUST-1 monoliths.¹⁶ Both MOF monoliths contain randomly distributed macropores.

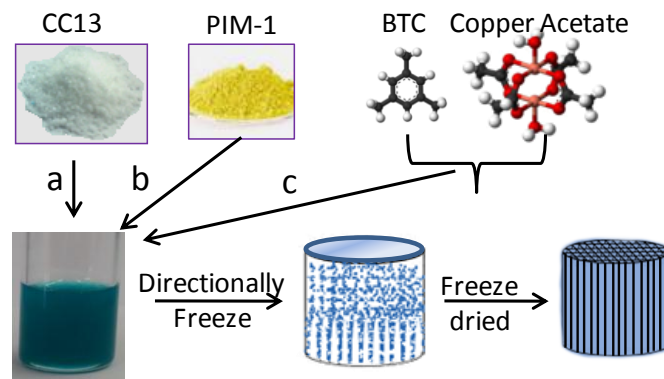


Fig. 1 The schematic representation of the procedures used for the preparation of aligned porous monoliths. Cage compound (a), polymer of intrinsic microporosity (b), or 1,3,5-benzene tricarboxylic acid (BTC) and copper acetate (c) are processed to form the monoliths, respectively. The colour of the solution varies depending on the type of solutes.

In this study, we demonstrate for the first time the preparation of aligned porous monoliths with intrinsic microporosity via a controlled freeze and freeze-drying approach, more specifically organic or metal-organic framework materials. By “intrinsic microporosity”, it means the material itself contains micropores and the micropores are not formed by templated synthesis or post-

treatment. The controlled freezing and freeze-drying approach is widely known as 'ice-templating', which has been used to prepare a wide range of porous materials and beyond.^{17,18} This templating method is highly versatile, advantageous for processes where heat-sensitive compounds are involved, and is unique in preparing aligned porous materials by orientating the growth of ice crystals during a directional freezing process.¹⁹ In addition to water, frozen organic solvents have also been used as templates, which may be termed as 'crystal templating'.¹⁹⁻²⁰ Here, the frozen-solvent-templating approach is applied to fabricate monoliths with aligned macropores and intrinsic micropores by directional freezing of chloroform solutions of CC & PIM and dimethyl sulfoxide (DMSO)-precursor solution and subsequent freeze-drying (Fig. 1).

We have chosen the organic cage compound CC13 for the preparation of aligned porous monolith due to its high solubility in dichloromethane/chloroform.²¹ A monolith can be readily formed (Fig. 2A inset) by directional freezing and freeze-drying of 200 mg cm⁻³ CC13-CHCl₃ solution, with distinguished aligned macropores (Fig. 2A & 2B). The macropore sizes are across a wide range with a peak size around 100 μm (Fig. 2C) and an intrusion pore volume of 1.19 cm³ g⁻¹ (Fig. S1). Because the pore structure is like aligned microchannels, it is difficult to clearly define the pore sizes as compared to the SEM images. As the monolith was prepared by a freeze-drying process, the crystallization of CC13 molecules during removal of the frozen solvent by sublimation was very limited, leading to an amorphous material (Fig. S2). This is consistent with the previous observations where freeze-drying the organic cage solutions (CC1 and CC3) led to the formation of amorphous solids.^{22,23} As this monolith was formed from small molecules (unlike polymers), the monolith was mechanically very weak.

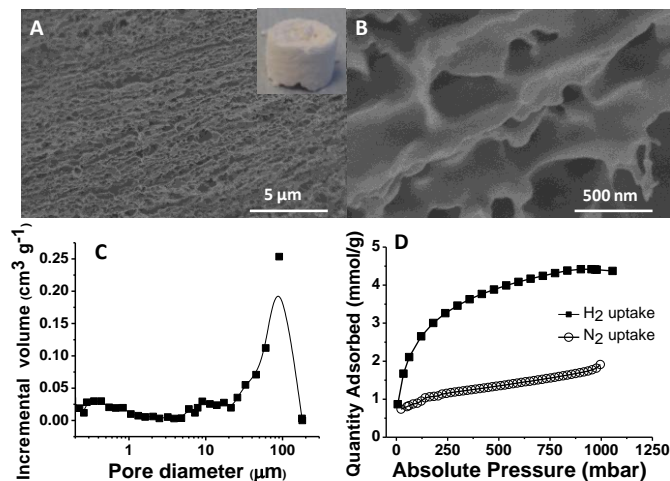


Fig. 2 The characterization data for the aligned CC13 monolith prepared from 200 mg cm⁻³ chloroform solution. (A-B) Scanning electron microscopic (SEM) images, (C) The macropore size distribution measured by Hg intrusion porosimetry, (D) The H₂ and N₂ uptake by the CC13 monolith measured at 77 K.

However, the amorphous organic cage solids formed by freeze-drying could exhibit significantly different porosity compared to the crystalline forms. For example, freeze-drying CC3 solutions led to the amorphous solid powders with much higher N₂ uptake and nearly doubled surface area. This was attributed to less efficient packing in the amorphous solid, resulting in lower density and additional extrinsic porosity.²² But in the case of CC1, the amorphous solid powder showed minimal N₂ uptake but an impressive uptake of H₂ ~ 4.5 mmol g⁻¹ at 77 K and 1 bar. Based on molecular dynamics (MD)

simulation, this was resulted from much less interconnected pore structure and smaller pores within the amorphous state.²³ Here, the freeze-dried CC13 monolith is an amorphous solid (Fig. S2). It shows a low N₂ uptake at 1.91 mmol g⁻¹ and with a surface area of 80 m² g⁻¹ (Fig. 2D), much lower than the crystalline CC13.²¹ When this material was re-dissolved in CHCl₃ and freeze-dried again, the resulting material showed a N₂ surface area of 5.0 m² g⁻¹ and N₂ uptake of only 0.15 mmol g⁻¹ (Fig. S3). However, like the freeze-dried amorphous CC1, the CC13 monolith gives a high H₂ uptake of 4.35 mmol g⁻¹ at 77 K and 1 bar (Fig. 2D). This may be explained by the similar structure of CC13 to CC1 in terms of relatively unfunctionalized vertex and racemic & flexible structure (Fig. S4). The porosity of the amorphous CC13 monolith to nitrogen is reduced, whereas the porosity to hydrogen is maintained, leading to improved selectivity. This is due to the constraining of the pathway through the structure by the loss of order, while the intrinsic porosity of the cages to guest molecules is maintained.²³

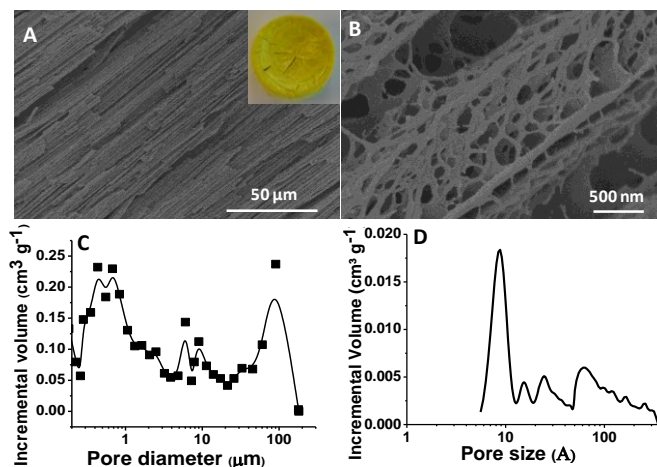


Fig. 3 The PIM-1 monolith prepared from 200 mg cm⁻³ PIM-1-chloroform solution. (A-B) SEM images, (C) Macropore size distribution as measured by Hg intrusion porosimetry, (d) Pore size distribution from N₂ sorption data.

PIM-1 has been extensively investigated.^{5,24} PIM-1 solution of 200 mg cm⁻³ in CHCl₃ was directionally frozen and freeze dried to produce a yellow monolith (Fig. 3A inset). This PIM-1 monolith is reasonably stiff with a Young modulus of 33 KPa (Fig. S5). The aligned feature (Fig. 3A) and the highly interconnected porous channel walls (Fig. 3B) can be clearly seen. As characterized by Hg intrusion porosimetry, the intrusion volume of this monolith is 4.21 cm³ g⁻¹ (Fig. S6). The intrusion volume at low pressures corresponds to large pores and the intrusion volume at high pressure for small pores. The intrusion profile reflects a wide pore size distribution with bimodal pore size peaks (Fig. 3C). The broad macropore size distribution particularly with the peak around 500 nm is consistent with the highly interconnected porous structure (Fig. 3B).

The isothermal adsorption curve of N₂ sorption is of a typical microporous material with a BET surface area of 766 m² g⁻¹ (Fig. S7). This material contains micropores and mesopores up to around 30 nm, with a sharp peak around 1 nm, calculated by the non-local density functional theory (NLDFT) (Fig. 3D). The macropores templated from frozen solvent may be readily tuned by simply changing the concentration of PIM-1 solution. For example, the monolith produced from 100 mg cm⁻³ PIM-1 solution also shows the aligned pore structures (Fig. S8) but with an increased intrusion volume of 5.41 cm³ g⁻¹. Both the shape of the cumulative intrusion volume curve and the macropore size distribution are similar to those of the PIM-1 monolith made from 200 mg cm⁻³ solution (Fig. S9).

In an effort to make aligned porous MOF monolith by directional freezing, we have selected the HKUST-1 as the model MOF. HKUST-1 has been prepared by various methods and investigated for different applications.^{6, 25-27} One of the attracting features is that HKUST-1 may be synthesized under mild conditions such as room temperature.²⁵⁻²⁶ Here, $\text{Cu}(\text{CH}_3\text{COO})_2 + 1,3,5\text{-benzene tricarboxylic acid (BTC)}$ solution was directionally frozen and freeze-dried to generate aligned porous HKUST-1 monolith. For the ease of freeze drying, DMSO (melting point 19 °C) was chosen over ethanol (melting point -114 °C) as solvent.

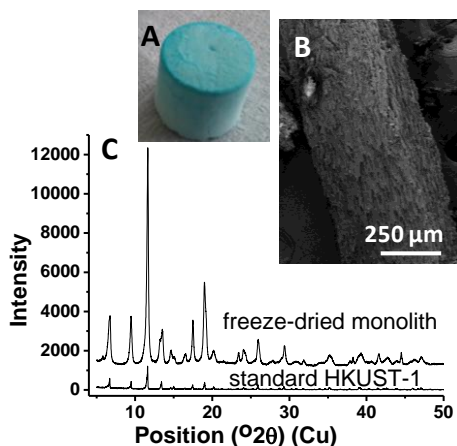


Fig. 4 The freeze-dried HKUST-1 monolith prepared from the heated DMSO solution at 80 °C for 24 hours. (A) The photo of the monolith, (B) The SEM image at low magnification, (C) The PXRD pattern of the monolith compared to that of the HKUST-1 particles prepared by the solvothermal method in water/ethanol.

The DMSO solution was prepared at room temperature and freeze-dried to produce a monolith. However, post-treatment in ethanol at 120 °C was required to improve the crystalline phase and the surface areas were lower than normal HKUST-1 (Fig. S10 – S14). However, when the DMSO solutions were heated to 80 °C, the monoliths with improved PXRD patterns were produced (Fig. S15). Fig. 4A shows a photograph of the monolith prepared. The aligned porous structure is across the whole monolith and is clearly revealed by low magnification SEM imaging (Fig. 4B), resembling the aligned structures prepared from other systems.^{17,19} The PXRD pattern is clean and sharp, consistent with the pattern of the HKUST-1 produced by the common solvothermal synthesis in water/ethanol mixture (Fig. 4C).²⁷ This demonstrates that a highly crystalline HKUST-1 monolith can be directly produced by freeze-drying warm DMSO solution without further post-treatment. This monolith is stable in ethanol or DMSO at least up to 120 °C but unstable when exposed to water.

The pore properties of this monolith are investigated further. The aligned pore structure is highly interconnected (Fig. 5A) and the pore surface is quite smooth (Fig. 5B). The N_2 sorption isotherm exhibits both characteristics of micropores (Fig. S16) and mesopores (Fig. 5C and the inset). This material has a surface area of $870 \text{ m}^2 \text{ g}^{-1}$ with a micropore volume of $0.406 \text{ cm}^3 \text{ g}^{-1}$ and mesopore volume of $0.271 \text{ cm}^3 \text{ g}^{-1}$. In addition, this porous monolith gives a high intrusion volume of $8.30 \text{ cm}^3 \text{ g}^{-1}$, contributed mainly from the aligned macropores (Fig. S17). The macropores show a bimodal size distribution with peaks around 10 μm (the aligned macropores) and 0.4 μm (pores in the wall) (Fig. 5D). During the freezing process, the size of solvent crystals could be varied readily by changing the freezing rates or freezing temperatures. As a result, the size of the aligned macropores could be tuned accordingly. With this freeze-

drying approach, the sizes of the macropores in the monoliths changed when the freezing temperatures were varied (Fig. S18). This freeze-drying approach from the precursor solution is unique in preparation of HKUST-1 monolith. Directly freeze-drying a HKUST-1 particle suspension could not produce a HKUST-1 monolith (Fig. S19 – S20).

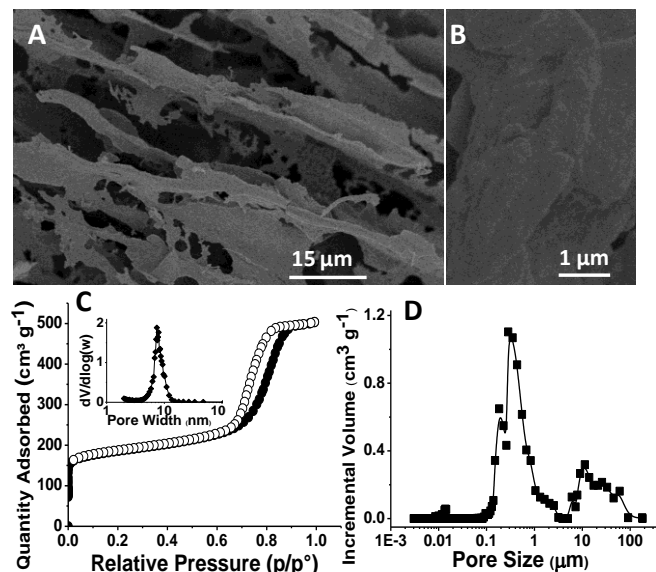


Fig. 5 Further pore characterization of the HKUST-1 monolith. (A–B) SEM images at high magnifications. (C) The N_2 sorption isothermal curves. The inset shows the mesopore size distribution. (D) Macropore size distribution from Hg intrusion porosimetry data.

Compared to the conventional porous monolith, the aligned porous monolith may provide low pressure drop.²⁸ This is important for column separation and continuous microreactors.^{29,30} The useful feature of the aligned pores was observed by the rate of absorption of liquid phase. The aligned pores in the HKUST-1 monolith could draw up liquid very fast while the absorption rate was very low when the aligned pores were parallel to the liquid phase surface (see Supporting Information). Further work is required to improve the mechanical stability of the monoliths but it has the potential for applications, *e.g.*, as monolithic catalyst support for continuous flow reactions with low pressure drop and maybe in general as monolithic reactors.^{9,29,30}

In conclusion, the frozen-solvent-templating approach has been successfully applied to fabricate aligned porous monoliths containing intrinsic micropores. Microporous organic cage compound CC-13 and polymer of intrinsic microporosity PIM-1 can be simply dissolved in chloroform and then freeze-dried to produce monoliths with highly interconnected aligned macropores while retaining the intrinsic micropores. It is also possible to produce the HKUST-1 monolith by freezing and freeze drying the warm DMSO precursor solution. The HKUST-1 monolith is highly crystalline, containing aligned macropores and intrinsic micropores. The aligned macropores in the monoliths may offer enhanced asymmetric mass transport and low pressure drop across the monolithic column. Such materials may be particularly advantageous for flow reaction or separation in a monolithic reactor or column.

Acknowledgements

The authors gratefully acknowledge the access to the facilities in the Centre for Materials Discovery at the University of Liverpool.

Notes and references

COMMUNICATION

Department of Chemistry, University of Liverpool, Oxford Street, Liverpool, L69 7ZD, UK. Email: zhanghf@liv.ac.uk

† Electronic Supplementary Information (ESI) available: experimental details, more PXRD and gas sorption data, SEM images, etc. See DOI: 10.1039/c000000x/

- 1 I. I. Ivanova and E. E. Knyazeva, *Chem. Soc. Rev.*, 2013, **42**, 3671; L. Tosheva and V. P. Valtchev, *Chem. Mater.*, 2005, **17**, 2494.
- 2 J. Biener, M. Stadermann, M. Suss, M.A. Worsley, M.M. Biener, K.A. Rose and T. F. Baumann, *Energy Environ. Sci.*, 2011, **4**, 656.
- 3 D. Wu, F. Xu, B. Sun, R. Fu, H. He, and K. Matyjaszewski, *Chem. Rev.*, 2012, **112**, 3959.
- 4 G. Zhang and M. Mastalerz, *Chem. Soc. Rev.*, 2014, **43**, 1924.
- 5 N. B. McKeown and P. M. Budd, *Chem. Soc. Rev.*, 2006, **35**, 675.
- 6 H.-C. Zhou, J. R. Long, and O. M. Yaghi, *Chem. Rev.*, 2012, **112**, 673.
- 7 P. Bernardo, E. Drioli and G. Golemme, *Ind. Eng. Chem. Res.*, 2009, **48**, 4638.
- 8 N. Stock and S. Biswas, *Chem. Rev.*, 2012, **112**, 933.
- 9 J. A. Moulijn and F. Kapteijn, *Curr. Opin. Chem. Eng.*, 2013, **3**, 346.
- 10 P. Küsgens, A. Zgaverdea, H.-G. Fritz, S. Siegle and S. Kaskel, *J. Am. Ceram. Soc.* 2010, **93**, 2476.
- 11 P. M. Budd, E. S. Elabas, B. S. Ghanem, S. Makhseed, N. B. McKeown, K. J. Msayib, C. E. Tattershall and D. Wang, *Adv. Mater.*, 2004, **16**, 456.
- 12 C. R. Mason, M. G. Buonomenna, G. Golemme, P.M. Budd, F. Galiano, A. Figoli, K. Friess and V. Hynek, *Polymer*, 2013, **54**, 2222.
- 13 A. F. Bushell, P. M. Budd, M. P. Attfield, J. T. A. Jones, T. Hasell, A. I. Cooper, P. Bernardo, F. Bazzarelli, G. Glarizia and J. C. Jansen, *Angew. Chem. Int. Ed.*, 2013, **52**, 1253.
- 14 O. Ardelean, G. Blanita, G. Borodi, M. D. Lazar, I. Misan, I. Goldea and D. Lupu, *Int. J. Hydrogen Energy* **2013**, **38**, 7046.
- 15 J.-B. Lin, R.-B. Lin, X.-N. Cheng, J.-P. Zhang and X.-M. Chen, *Chem. Commun.*, 2011, **47**, 9185.
- 16 A. Ahmed, M. Forster, P. Myers and H. Zhang, *Chem. Commun.*, 2014, **50**, 14314.
- 17 L. Qian and H. Zhang, *J. Chem. Technol. Biotechnol.* 2011, **86**, 172-184.
- 18 S. Deville, *J. Mater. Res.*, 2013, **28**, 2202.
- 19 H. Zhang, I. Hussain, M. Brust, M. F. Butler, S. P. Rannard and A. I. Cooper, *Nature Mater.*, 2005, **4**, 787.
- 20 C. Guizard, J. Leloup and S. Deville, *J. Am. Ceram. Soc.*, 2014, **97**, 2020.
- 21 T. Hasell, J. L. Culshaw, S. Y. Chong, M. Schmidtman, M. A. Little, K. E. Jelfs, E. O. Pyzer-Knapp, H. Shepherd, D. J. Adams, G. M. Day and A. I. Cooper, *J. Am. Chem. Soc.*, 2014, **136**, 1438.
- 22 T. Hasell, S. Y. Chong, K. E. Jelfs, D. J. Adams and A. I. Cooper, *J. Am. Chem. Soc.*, 2012, **134**, 588.
- 23 S. Jiang, K. E. Jelfs, D. Holden, T. Hasell, S. Y. Chong, M. Haranczyk, A. Trewin and A. I. Cooper, *J. Am. Chem. Soc.*, 2013, **135**, 17818.
- 24 P. M. Budd, B. S. Ghanem, S. Makhsee, N. B. McKeown, K. J. Msayib and C. E. Tattershall, *Chem. Commun.*, 2004, 230.
- 25 J. Huo, M. Brightwell, S. E. Hanakri, A. Garai and D. Bradshaw, *J. Mater. Chem. A* 2013, **1**, 15220.
- 26 G. Majano and J. Pérez-Ramirez, *Adv. Mater.*, 2013, **25**, 1052.
- 27 A. Ahmed, M. Forster, R. Clowes, D. Bradshaw, P. Myers and H. Zhang, *J. Mater. Chem. A*, 2013, **1**, 3276.
- 28 A. Ahmed, P. Myers and H. Zhang, *Anal. Methods.*, 2012, **4**, 3942-3947.
- 29 S. Roy, T. Bauer, M. Al-Dahhan, P. Lehner and T. Turek, *AICHE J.*, 2004, **50**, 2918.
- 30 E.V. Ramos-Fernandez, M. Garcia-Domingos, J. Juan-Alcaniz, J. Gascon and F. Kapteijn, *Appl. Catal. A* 2011, **39**, 1261.